

Article

Research on Ultra-Low-Frequency Communication Based on the Rotating Shutter Antenna

Faxiao Sun ^{1,2,3} , Feng Zhang ^{1,2,*}, Xiaoya Ma ^{1,2,3}, Zhaoqian Gong ^{1,2}, Yicai Ji ^{1,2,3} and Guangyou Fang ^{1,2,3}

¹ Aerospace Information Research Institute, Chinese Academy of Sciences, Beijing 100190, China; sunfaxiao19@mails.ucas.ac.cn (F.S.); maxiaoya20@mails.ucas.ac.cn (X.M.); zqgong@mail.ie.ac.cn (Z.G.); ycji@mail.ie.ac.cn (Y.J.); gyfang@mail.ie.ac.cn (G.F.)

² Key Laboratory of Electromagnetic Radiation and Sensing Technology, Chinese Academy of Sciences, Beijing 100190, China

³ School of Electronic, Electrical and Communication Engineering, University of Chinese Academy of Sciences, Beijing 100049, China

* Correspondence: zhangfeng002723@aircas.ac.cn

Abstract: This paper proposes a rotating shutter antenna that can directly generate 2FSK signals in the ULF band and it is expected to be used as the transmitter for magnetic induction (MI) underground communication systems. The antenna was modeled using ANSYS Maxwell and the magnetic field distribution was simulated. The results show that the interaction between the high-permeability shutter and the mutual cancellation of magnets decreased the transmitting magnetic moment of the antenna. A prototype antenna was manufactured and the time and frequency properties of the measured B_z field were the same as the simulated results, while the magnitude of the measured signal was larger. The propagation characteristics of the antenna in air–soil–rock were simulated using FEKO and the results show that the signal strength was greater than 1 fT at a depth of 450 m from the antenna whose magnetic moment as 1 Am^2 . The relationship between different magnetic components and azimuth could be used to enhance the signal strength. The formula of the B_z field was derived using the measured magnitude versus distance and the path loss was also analyzed. Finally, the 2FSK modulation property of the antenna was verified by indoor communication experiments with a code rate of 12.5 bps in the ULF band.

Keywords: ultra-low-frequency communication; mechanical antenna; layered media; rotating shutter antenna



Citation: Sun, F.; Zhang, F.; Ma, X.; Gong, Z.; Ji, Y.; Fang, G. Research on Ultra-Low-Frequency Communication Based on the Rotating Shutter Antenna. *Electronics* **2022**, *11*, 596. <https://doi.org/10.3390/electronics11040596>

Academic Editor: Naser Ojaroudi Parchin

Received: 6 January 2022

Accepted: 14 February 2022

Published: 15 February 2022

Publisher's Note: MDPI stays neutral with regard to jurisdictional claims in published maps and institutional affiliations.



Copyright: © 2022 by the authors. Licensee MDPI, Basel, Switzerland. This article is an open access article distributed under the terms and conditions of the Creative Commons Attribution (CC BY) license (<https://creativecommons.org/licenses/by/4.0/>).

1. Introduction

The electromagnetic waves at radio frequencies have short wavelengths and poor penetrating capabilities, which make them lose part of their energy in a complex electromagnetic environment [1]. For example, the permittivity and conductivity of soil have a great relationship with the water content, which causes significant attenuation of high-frequency electromagnetic waves. This leads to the fact that radio-frequency communication cannot be widely used in underground communication. To overcome this problem, magnetic induction communication technology with ultra-low-frequency magnetic fields is widely used in underground communication, such as Through-The-Earth communication [2]. The permeability of non-magnetic materials is almost the same, which provides a relatively stable channel for the propagation of magnetic field signals and the stable channel enables the magnetic induction communication to avoid the shortcomings of multipath propagation, large propagation delay and high bit error rate of acoustic transmission through the ground [3].

Normally, magnetic inductive communication systems use coils to generate and receive magnetic field signals in near-field zone [4]. However, in the ultra-low-frequency band, the

size of the coil is also very large, which brings great inconvenience to the placement and layout of the system [5,6].

To overcome the shortcomings of traditional low-frequency antennas, such as large size, low efficiency and high-power consumption, in 2017, the US Department of Defense Advanced Research Project Agency (DARPA) proposed the AMEBA plan [7]. Different from traditional antennas, AMEBA mainly generates alternating electromagnetic waves directly through electrical charges or magnetic moments in mechanical motion, which is a process of converting mechanical energy into electromagnetic energy [8,9]. As a kind of mechanical antenna, the rotating permanent magnet antenna (RPMA) drives the permanent magnet to rotate so as to obtain an alternating magnetic field. It is likely to be used as the transmitting antenna in the magnetic induction communication system.

After AMEBA was proposed, many researchers have become interested in RPMA and began to study it, including field generation and measurement [10,11] and radiation power analysis [12]. Skyler Selvin et al. analyzed the efficiency of RPMA and proposed a method to build an RPMA array to improve antenna efficiency [13]. Srinivas Prasad M.N. et al. proposed a prototype consisting of an array of magnetic pendulums in oscillatory motion at ULF. The transmission efficiency of the magnetic pendulums array is higher than a bare coil through the measurement in the near field [14,15].

The communication system which uses RPMA as the transmitter mostly adopts direct antenna modulation (DAM). For example, we can obtain an OOK signal by controlling the driver switch and an FSK signal by controlling the speed of motion [16–20]. Besides, Refs. [21–24] proposed that amplitude and phase modulation can be achieved by using an external modulator. However, these methods require additional energy to control the modulator in real time, which is difficult to implement.

To effectively avoid the limitation of the motor to the antenna's operating frequency range, we used a rotating shutter antenna as our transmitting antenna, which could obtain a magnetic field signal that is four times the rotating frequency. ANSYS Maxwell was used to analyze the magnetic field distribution of the rotating shutter antenna and the results show that the interaction between the high-permeability shutter and the mutual cancellation of magnets decreased the transmitting magnetic moment. A prototype antenna was manufactured and the experimental results are in great agreement with the simulated results, while the magnitude of the measured signal was larger. FEKO was used to analyze the propagation characteristics of the RPMA in air–soil–rock media and the simulated results show that the B_z -field at a depth of 450 m away from the antenna on ground with a magnetic moment of 1 Am^2 was 1 fT. The formula of the B_z -field was derived using measured magnitude versus distance and the path loss was also analyzed. The formula shows that the path loss of the rotating shutter antenna in free space was 303 dB at a distance of 570 m, while the signal strength was 1 fT. The prototype antenna was also used to carry out indoor communication experiments with a code rate of 12.5 bps in the ULF. This paper is organized as follows: In Section 2, the principle and simulation of the rotating shutter antenna are presented. The simulation of RPMA in layered media is shown in Section 3. In Section 4, the prototype and the experimental results are presented. Finally, Section 5 draws the conclusion.

2. Principle and Simulation of the Rotating Shutter Antenna

The radiation principle of the rotating permanent magnet antenna can be summarized as follows: the motor drives the magnet to rotate so that its static magnetic field is converted to an alternating magnetic field. The corresponding relationship between the signal frequency and the motor speed n can be expressed as

$$f = \frac{n}{60} \quad (1)$$

When the speed n of the drive motor is greater than 18,000 rpm, the frequency of the signal obtained is greater than 300 Hz, which is difficult for common servo motors on the market.

The rotating shutter antenna was proposed by M. Golkowski in 2018 [25] and the prototype mainly consists of magnets and a shutter made of soft magnetic materials, such as permalloy, whose relative permeability is significant. Assuming that the number of openings is N , the antenna needs two N magnets of different polarities which are alternately placed to form a circle. During the working process, the shutter rotates to block the permanent magnets of different polarities to generate an altering magnetic field, whose frequency is N times the rotating fundamental frequency. The relationship between frequency and speed can be expressed as

$$f = \frac{n}{60} \cdot N \tag{2}$$

Compared with RPMA, the rotating shutter antenna can reduce the speed to n/N . The block diagram of the antenna principle when $N = 4$ is shown in Figure 1.

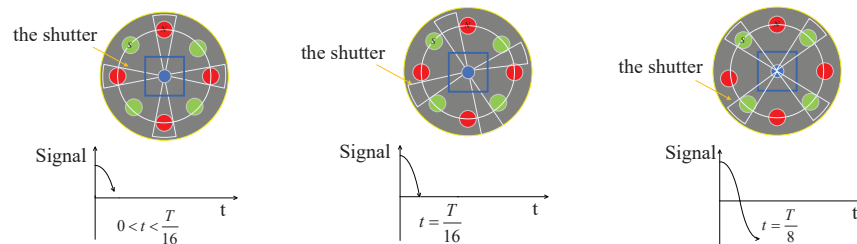


Figure 1. Block diagram of the rotating shutter antenna when $N = 4$.

ANSYS Maxwell was used to analyse a rotating shutter antenna with $N = 4$; the parameters of the simulation are shown in Table 1. A free-space sphere with a radius of 4 m was established and the boundary adopted natural boundary conditions, which made the magnetic field continuous inside and outside the simulation area. The magnetic field produced by the permanent magnets was used as excitation and the effects of eddy current induced on the shutter were considered. Regardless of mechanical damping, a band area with a set rotation speed of 4800 rpm was used to simulate the rotation of the shutter, which corresponded to a fundamental rotation frequency of 80 Hz, so the frequency of the magnetic field signal was, theoretically, 320 Hz.

Table 1. The parameters of the simulation.

Parameters	Values	Parameters	Values
radius of the magnet	10 mm	magnetic remanence	1.47 T
height of the magnet	100 mm	thickness of the shutter	1.5 mm
openings of the shutter	4	rotating speed	4800 rpm

We placed a point at the position of 3 m in the axial direction of the rotating shutter antenna and obtained the B_z -field. The simulated results are shown in Figure 2. Figure 2a shows the signal with an amplitude of 3.5 nT at the point 3 m away from the transmitter, which is much smaller than the theoretical value. The corresponding spectrogram is shown in Figure 2b, which represents B_z -field strength as a function of time and frequency. It can be clearly seen the signal whose frequency is 320 Hz in the spectrogram and multiple harmonics are visible.

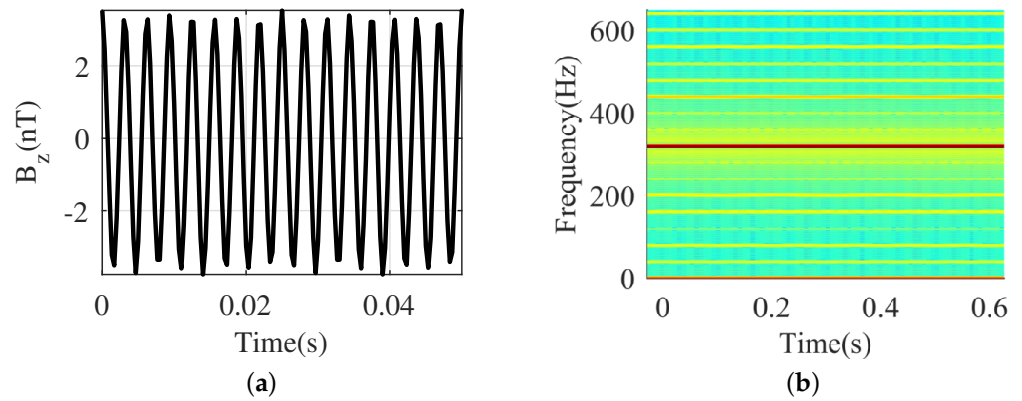


Figure 2. (a) Field at the point 3 m away from the shutter antenna. (b) Spectrogram of field.

The magnetic field intensity distribution on the rotating shutter at different times is shown in Figure 3. It is clear that a large part of the energy was concentrated on the shutter, which may be one of the reasons for the field strength being smaller than the theoretical calculation.

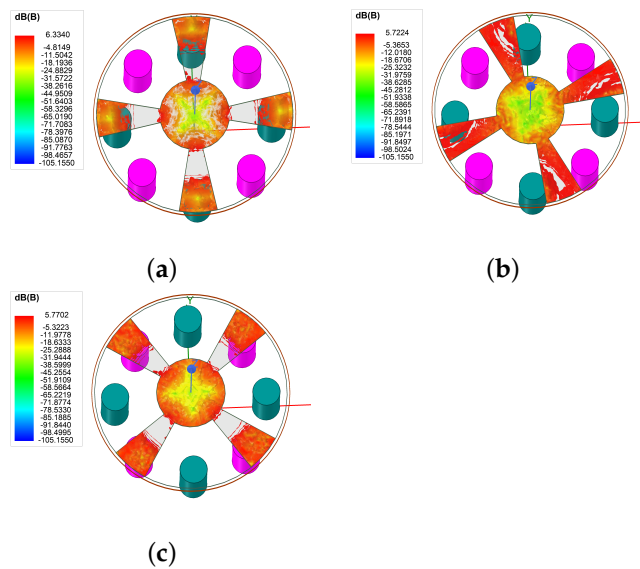


Figure 3. B-field distribution on the rotating shutter at different times: (a) $t = 0$ s; (b) $t = 0.667$ ms; (c) $t = 1.67$ ms.

The side view and top view of the distribution of the B-field by intercepting different planes in the simulation are shown in Figure 4. The fast attenuation of the signal can be ascribed to both the interaction of the high-permeability shutter and the mutual cancellation of magnets.

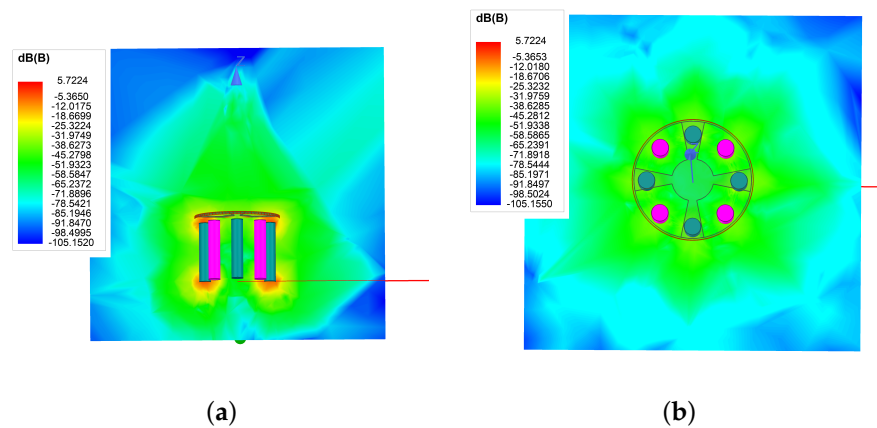


Figure 4. B-field distribution from different viewing angles: (a) side view; (b) top view.

3. Propagation Characteristics in Layered Media

It is promising that RPMA can be used as the transmitting antenna in magnetic inductive underground communication and it is particularly important to study the radiation characteristics of RPMA in layered media. Layered media cause interface emission loss and transmission medium loss because of different permittivity and conductivity.

This paper used FEKO to construct an equivalent model of a rotating permanent magnet antenna that rotated vertically on the ground and analyzed its magnetic field characteristics in three-layer media, such as air–soil–rock. The simulation parameters are shown in Table 2.

Table 2. The parameters of the simulation.

	Parameters	Values
antenna	frequency	320 Hz
	moment	1 Am ²
	depth	1500 m
soil	permittivity	10
	conductivity	0.01 S/m
rock	permittivity	10
	conductivity	0.01 S/m

The curves of magnetic flux intensity versus distance are shown in Figure 5 and it is clear that the maximum penetrating depth could reach 450 m for magnetic induction communication.

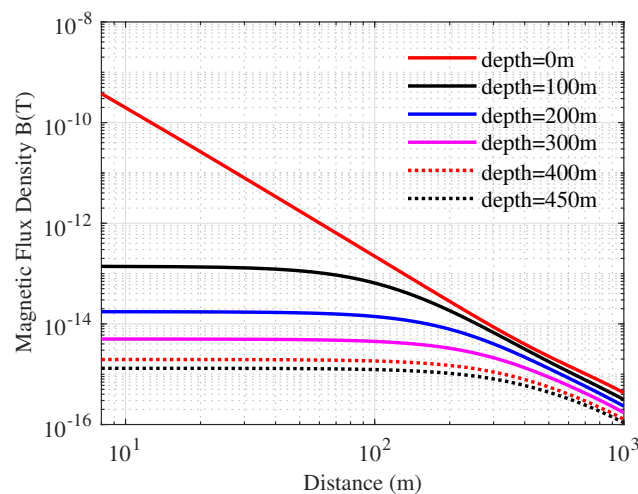


Figure 5. Change in magnetic flux density with the distance at different depths.

The curves of B_r and B_ϕ with azimuth at different depths shown in Figure 6 show that, at the same depth, the phase between the two magnetic field components was constant. If we used a two-axis magnetic field sensor to receive, we could obtain an enhanced signal by shifting the ϕ -direction component with a constant phase and then adding it to the r -direction component.

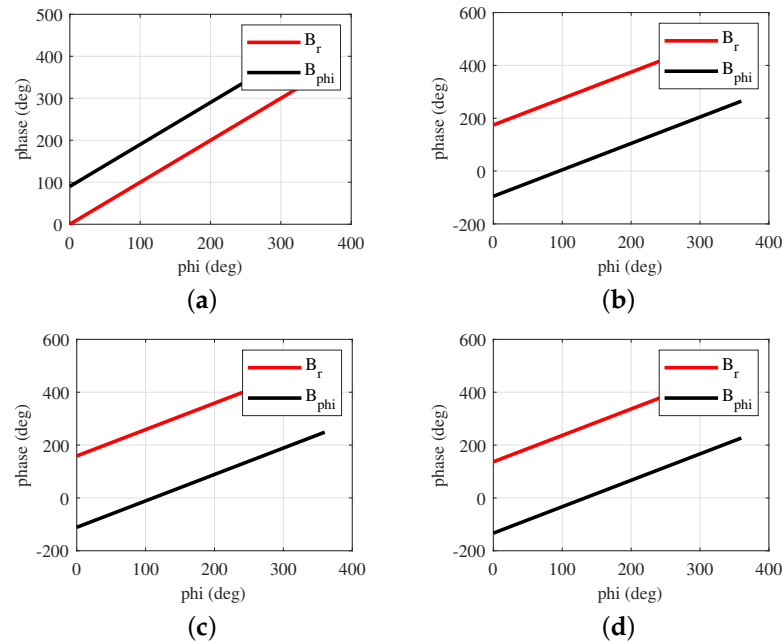


Figure 6. Change in B_r and B_ϕ with azimuth at different depths: (a) depth = 0 m; (b) depth = 150 m; (c) depth = 300 m; (d) depth = 450 m.

4. Experimental Results

The experimental results are presented in two sub-sections, i.e., (a) measurement of the rotating shutter antenna and (b) communication based on the rotating shutter antenna.

4.1. Measurement of the Rotating Shutter Antenna

A prototype, as shown in Figure 7, with the same size as shown in Table 2 was manufactured and magnets were fixed on an aluminum plate through an aluminum alloy cover. The YASKAWA servo AC motors with model SGM7J-01AFC6S were used as the driver, which could provide a rated torque of 637 mN·m and a rated power of 200 W. The rotation axis of the shutter antenna and the ULF receiver shown in Figure 8 were placed in line to measure the B_z -field. The distance between the antenna and the receiver was 3 m, as that in simulation. In the communication experiment, the information symbols were sent to the servo through software named MPE720 Ver. 7 to control the rotating shutter antenna in real time.

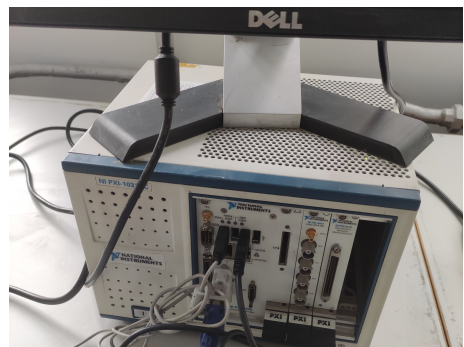
The portable ULF receiver, shown in Figure 8, consisted of a magnetic sensor and an NI collector. The conversion coefficient of the magnetic sensor was 8 mV/nT, so we could directly convert the received voltage signal into field strength. The NI collector was utilized to digitize and store the received signal with a sampling rate of 3 Ksps.



Figure 7. The rotating shutter antenna.



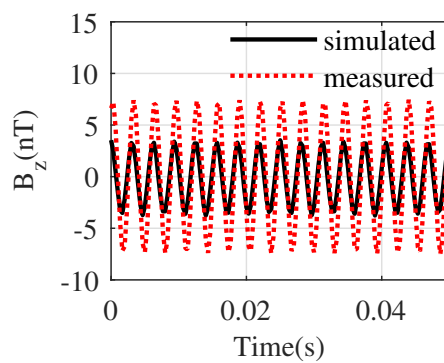
(a)



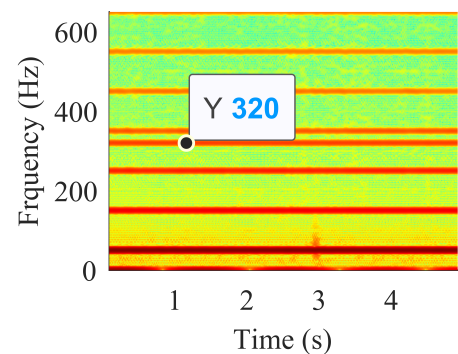
(b)

Figure 8. ULF receiver: (a) magnetic sensor; (b) NI sampler.

The measured result shown in Figure 9 shows that, when the motor speed was set to 4800 rpm, the frequency of the signal obtained was in good agreement with the simulated result, but the amplitude was larger than that obtained in the simulation, which may be ascribed to the fact that the material in the simulation was not consistent with our prototype and the metal substances in the experimental environment may also have had a certain influence on the signal strength. From the spectrogram of the field shown in Figure 9b, we can clearly see the 320 Hz signal.



(a)



(b)

Figure 9. (a) Field at the point 3 m away from the shutter antenna. (b) Spectrogram of field.

We measured the B_z -field by placing the receiving antenna along the axis direction of the rotating shutter antenna and changing the distance between them (such as 0.6 m, 1.2 m, ..., 4.8 m and 5.4 m); the variation in the field strength with distance is shown in Figure 10. The propagation characteristic curve was fitted using MATLAB and the result is also shown in Figure 10. The fitting curve can be expressed as

$$B_z(\text{nT}) = \frac{188}{r^3} \quad (3)$$

The intensity of the B_z -field is inversely proportional to the third power of the distance, which is in line with the attenuation law of the near-field signal. However, different from the rotating permanent magnet antennas ($B_z = \frac{\mu m}{2\pi r^3}$), the expression of the magnetic flux density of the rotating shutter antenna shown in Equation (3) cannot find the similar law related to the magnetic moment.

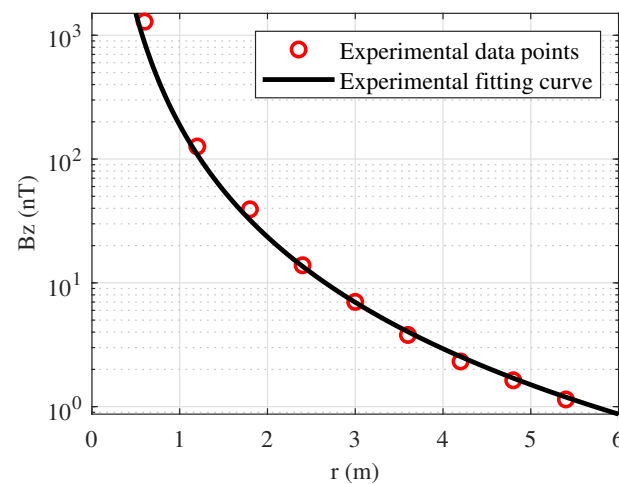


Figure 10. The change in B_z -field with distance.

In MI communication, the rotating shutter antenna is used as the transmitter. The path loss can be defined as

$$PL = 20 \lg \frac{B_r}{B_z} \approx 137.4 + 60 \lg(r) \quad (4)$$

where B_r is the remanence of the permanent magnet and B_z is given in Equation (3).

The path loss determined by the propagation range was simulated, as shown in Figure 11. The point with path loss of 303 dB (the received magnetic field was about 1 fT for $B_r = 1.4\text{T}$) is marked with red lines in Figure 11. If the receiver can handle magnetic field signals of 1 fT, the MI communication distance of up to 570 m could be achieved. The antenna prototype shown in Figure 7 was equivalent to an RPMA with a transmitting magnetic moment of 0.94 Am^2 . If the antenna was used as the transmitting antenna in the magnetic induction communication, a two-unit antenna array would be required to make the maximum detection depth reach 450 m. The synchronization between the elements would also be difficult. Searching for a new method to enhance magnetic moments will be the focus of our research work.

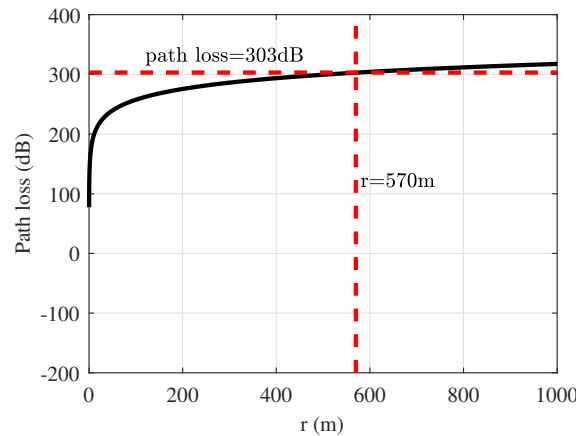


Figure 11. Path loss versus propagation range.

4.2. Communication Based on the Rotating Shutter Antenna

We changed the distance between the transmitter and the receiver antenna to 4.5 m, while the other experimental parameters were the same as those mentioned above. Using control software to rotate the motor between 4800 rpm and 4950 rpm, we theoretically obtained 320 Hz and 330 Hz signals, which can represent different binary information symbols such as ‘1’ and ‘0’. The time required for the motor to switch between different speeds was set to 100 ms and the time for a constant rotation was 80 ms, which determined the code rate of communication.

The modulated signal after bandpass filtering is shown in Figure 12a. Its corresponding spectrum, shown in Figure 12b, demonstrates that the frequency of the 2FSK signal did not reach the theoretical value, which may have been due to insufficient control accuracy. In addition, there was a very obvious frequency component between the frequency spectra of the 303.7 Hz and 316.2 Hz signals, which was introduced during the motor speed switching process. This problem could be solved by increasing the constant speed time of the motor, but this would reduce the communication code rate.

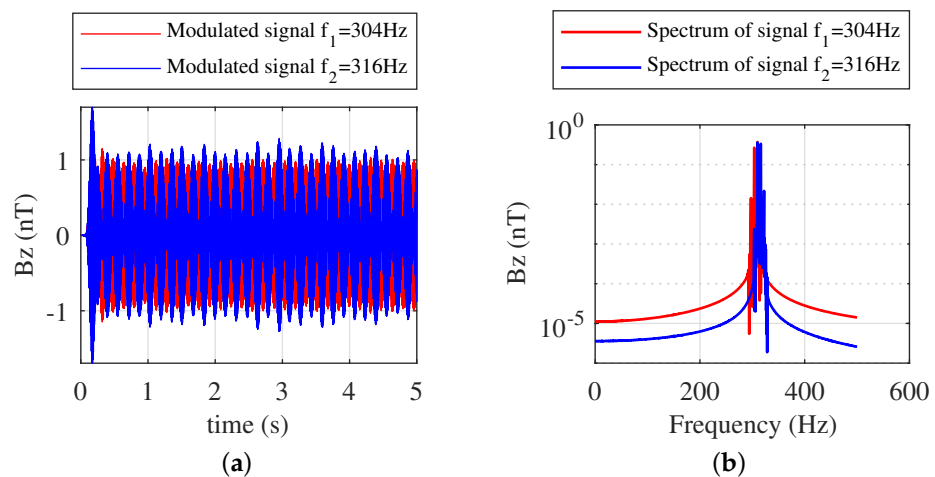


Figure 12. (a) Modulated signals at the point 5.4 m away from the rotating shutter antenna; (b) spectrum of signals.

It can be clearly observed from the spectrogram shown in Figure 13a that the signals with frequencies of 303.7 Hz and 316.2 Hz appeared alternately in sequence, which means that the information symbol ‘1010101...’ was received. The received signal is processed by filtering out the power–frequency signal, passing through bandpass filtering and extracting the envelope of the filtered signal; then, the information symbol shown in Figure 13b can

be obtained through amplitude judgment. It was found, from the demodulated information, that there were 12.5 symbols in one second, which means that the code rate of communication was 12.5 bps.

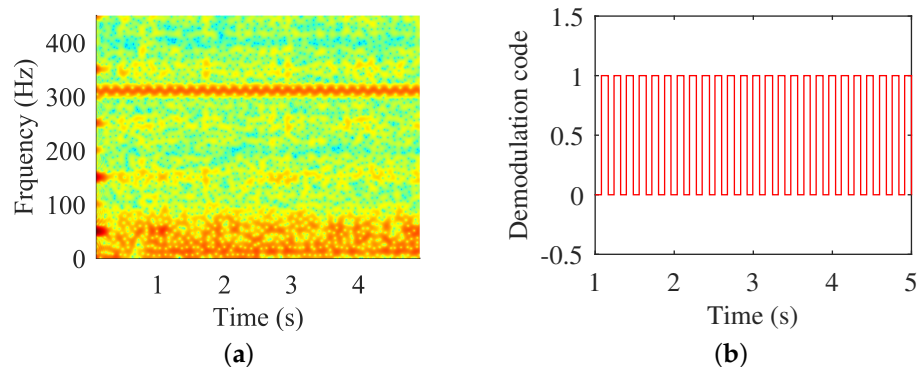


Figure 13. (a) Spectrogram of 2FSK signal; (b) demodulated code.

Table 3 summarizes the performance comparison between the previously proposed systems and the system adopted in this paper. It can be found that the frequency of the signal, the communication rate and the communication distance could not be taken into account simultaneously in the existing research study. Our system mainly considers a higher communication code rate, but the communication range was not the longest, which is also a focus for our future research work.

Table 3. Performance comparison of rotating permanent magnet antennas.

Reference	Frequency	Data Rate	Detection Distance
Ref. [10]	500 Hz	/	<130 m
Ref. [11]	22 Hz	8 bps	0.7 m
Ref. [14]	1.03 kHz	2 bps	30 m
Ref. [17]	100 Hz	0.25 bps	5 m
Ref. [20]	30 Hz	5 bps	100 m
Ref. [22]	40 Hz	<2 bps	5 m
Ref. [23]	50 Hz	40 bps	0.25 m
Our work	320 Hz	12.5 bps	5 m

Since the antenna operates in its near-field region, the signal strength decays with the third power of the distance, which limits the maximum communication distance of the communication system. Similarly, due to the low carrier frequency of the system, the data rate cannot be too high, which limits the diversity of communication. For example, the communication rate is only suitable for message transmission. In addition, an array with more shutter antennas would be a good choice to increase the magnetic moment, but assuring the control accuracy of the motor would be necessary and difficult to achieve.

5. Conclusions

This paper used ANSYS Maxwell to analyze the magnetic field distribution of the rotating shutter antenna and the results show that the interaction between the high-permeability shutter and the mutual cancellation of magnets decreased the transmitting magnetic moment. A prototype was manufactured; the measured results are in great agreement with the simulated results, while the magnitude of the measured signal was larger. We used FEKO to analyze the propagation characteristics of RPMA in air–soil–rock and the simulated results show that the signal strength was greater than 1 fT at a depth of 450 m from the antenna, whose moment was 1 Am². Since the phase difference between B_r and B_ϕ remained constant at $\pm 90^\circ$, we could use a multi-directional receiver to receive the multi-directional field components; then, the signal strength could be enhanced by shifting

the phases of the B_r -field component and adding it to another component, such as a B_ϕ -field component. The formula shows that the path loss of the rotating shutter antenna at 570 m was 303 dB, which means that the signal strength was 1 fT. The rotating shutter antenna was equivalent to an RPMA with a transmitting magnetic moment of 0.94 Am^2 . If the antenna was used as the transmitting antenna in the magnetic induction communication, a two-element antenna array would be required to make the maximum detection depth reach 450 m. The synchronization between the elements would make the control of the system very difficult. Finding a new method to increase the transmitting magnetic moment and the synchronization of the elements will be the focus of our next research studies. FSK modulation could be realized by controlling the motion state of the motor and the constant time of the motor determined the symbol rate. The prototype was used to achieve indoor communication with a code rate of 12.5 bps in the ULF.

Author Contributions: Conceptualization, F.S., X.M. and F.Z.; methodology, F.S. and X.M.; software, F.S. and Z.G.; validation, F.S. and F.Z.; formal analysis, F.S.; investigation, F.S. and X.M.; resources, Y.J.; data curation, F.Z. and Z.G.; writing—original draft preparation, F.S.; writing—review and editing, F.Z. and Y.J.; visualization, F.S.; supervision, G.F.; project administration, Y.J.; funding acquisition, G.F. All authors have read and agreed to the published version of the manuscript.

Funding: This research study was funded by the National Natural Science Foundation of China, grant number 61827803.

Institutional Review Board Statement: Not applicable.

Informed Consent Statement: Not applicable.

Data Availability Statement: Not applicable.

Conflicts of Interest: The authors declare no conflict of interest.

References

1. Kilinc, D.; Akan, O.B. Nanoscale magneto-inductive communication. In Proceedings of the 2013 Asilomar Conference on Signals, Systems and Computers, Pacific Grove, CA, USA, 3–6 November 2013; pp. 1061–1065.
2. Yan, L.; Waynert, J.; Sunderman, C.; Damiano, N. Statistical analysis and modeling of VLF/ELF noise in coal mines for through-the-earth wireless communications. In Proceedings of the 2014 IEEE Industry Application Society Annual Meeting, Vancouver, BC, Canada, 5–9 October 2014; pp. 1–5.
3. Domingo, M.C. Magnetic Induction for Underwater Wireless Communication Networks. *IEEE Trans. Antennas Propag.* **2012**, *60*, 2929–2939. [[CrossRef](#)]
4. Sun, Z.; Akyildiz, I.F. Magnetic Induction Communications for Wireless Underground Sensor Networks. *IEEE Trans. Antennas Propag.* **2010**, *58*, 2426–2435. [[CrossRef](#)]
5. Gulbahar, B.; Akan, O.B. A communication theoretical modeling and analysis of underwater magneto-inductive wireless channels. *IEEE Trans. Wireless Commun.* **2010**, *11*, 3326–3334. [[CrossRef](#)]
6. Akyildiz, I.F.; Wang, P.; Sun, Z. Realizing underwater communication through magnetic induction. *IEEE Commun. Mag.* **2015**, *53*, 42–48. [[CrossRef](#)]
7. Ding, H. DARPA mechanical antenna project may set off a military communications revolution. *Commilit* **2017**, *26*, 71–73.
8. Bickford, J.A.; McNabb, R.S.; Ward, P.A.; Freeman, D.K.; Weinberg, M.S. Low frequency mechanical antennas: Electrically short transmitters from mechanically-actuated dielectrics. In Proceedings of the 2017 IEEE International Symposium on Antennas and Propagation & USNC/URSI National Radio Science Meeting, San Diego, CA, USA, 9–14 July 2017; pp. 1475–1476.
9. Manteghi, M. A navigation and positioning system for unmanned underwater vehicles based on a mechanical antenna. In Proceedings of the 2017 IEEE International Symposium on Antennas and Propagation & USNC/URSI National Radio Science Meeting, San Diego, CA, USA, 9–14 July 2017; pp. 1997–1998.
10. Burch, H.C.; Garraud, A.; Mitchell, M.F.; Moore, R.C.; Arnold, D.P. Experimental Generation of ELF Radio Signals Using a Rotating Magnet. *IEEE Trans. Antennas Propag.* **2018**, *66*, 6265–6272. [[CrossRef](#)]
11. Fawole, O.C.; Tabib-Azar, M. An Electromechanically Modulated Permanent Magnet Antenna for Wireless Communication in Harsh Electromagnetic Environments. *IEEE Trans. Antennas Propag.* **2017**, *65*, 6927–6936. [[CrossRef](#)]
12. Bickford, J.A.; Duwel, A.E.; Weinberg, M.S.; McNabb, R.S.; Freeman, D.K.; Ward, P.A. Performance of Electrically Small Conventional and Mechanical Antennas. *IEEE Trans. Antennas Propag.* **2019**, *67*, 2209–2223. [[CrossRef](#)]
13. Selvin, S.; Srinivas, P.M.N.; Huang, Y.; Wang, E. Spinning magnet antenna for VLF transmitting. In Proceedings of the 2017 IEEE International Symposium on Antennas and Propagation & USNC/URSI National Radio Science Meeting, San Diego, CA, USA, 9–14 July 2017; pp. 1477–1478.

14. Srinivas, P.M.N.; Tok, R.U.; Wang, Y.E. Magnetic pendulum arrays for ULF transmission. In Proceedings of the 2018 IEEE International Symposium on Antennas and Propagation & USNC/URSI National Radio Science Meeting, Boston, MA, USA, 8–13 July 2018; pp. 71–72.
15. Srinivas, P.M.N.; Fereidoony, F.; Wang, Y.E. 2D Stacked magnetic pendulum arrays for efficient ULF transmission. In Proceedings of the 2020 IEEE International Symposium on Antennas and Propagation and North American Radio Science Meeting, Montreal, QC, Canada, 5–10 July 2020; pp.1305–1306.
16. Liu, Y.; Hou, M.; Gong, S. A Rotating Permanent magnet transmitter for magnetic induction communication in RF-impenetrable environment. In Proceedings of the 2020 IEEE MTT-S International Conference on Numerical Electromagnetic and Multiphysics Modeling and Optimization (NEMO), Hangzhou, China, 7–9 December 2020; pp.1–3.
17. Glickstein, J.S.; Liang, J.; Choi, S.; Madanayake, A.; Mandal, S. Power-efficient ELF wireless communications using electro-mechanical transmitters. *IEEE Access* **2020**, *8*, 2455–2471. [[CrossRef](#)]
18. Tarek, M.T.B.; Dharmasena, S.; Madanayake, A.; Choi, S.; Glickstein, J.; Liang, J.; Mandal, S. Power-efficient data modulation for all-mechanical ULF/VLF transmitters. In Proceedings of the 2018 IEEE 61st International Midwest Symposium on Circuits and Systems (MWSCAS), Windsor, ON, Canada, 5–8 August 2018; pp.759–762.
19. Cao, J.; Liu, Y.; Gong, S. Low frequency mechanical antenna for underwater communication. In Proceedings of the 2019 International Conference on Electronic Engineering and Informatics (EEI), Nanjing, China, 8–10 November 2019; pp.140–142.
20. Liu, Y.; Gong, S.; Liu, Q.; Hou, M. A Mechanical Transmitter for Undersea Magnetic Induction Communication. *IEEE Trans. Antennas Propag.* **2021**, *69*, 6391–6400. [[CrossRef](#)]
21. Strachen, N.D.; Booske, J.H.; Behdad, N. Mechanical Super-Low Frequency (SLF) transmitter using electrically-modulated reluctance. In Proceedings of the 2018 IEEE International Symposium on Antennas and Propagation & USNC/URSI National Radio Science Meeting, Boston, MA, USA, 8–13 July 2018; pp.67–68.
22. Zhang, J.; Song, Z.; Zhang, D.; Xi, X. Amplitude modulation method of the mechanically rotating-based antenna. *Electron. Lett.* **2020**, *56*, 321–323 [[CrossRef](#)]
23. Barani, N.; Sarabandi, K. A phase modulation scheme for super-low frequency handheld mechanical antennas. In Proceedings of the 2020 IEEE International Symposium on Antennas and Propagation and North American Radio Science Meeting, Montreal, QC, Canada, 5–10 July 2020; pp.467–468.
24. Barani, N.; Sarabandi, K. A frequency multiplier and phase modulation approach for mechanical antennas operating at Super Low Frequency (SLF) Band. In Proceedings of the 2019 IEEE International Symposium on Antennas and Propagation and USNC-URSI Radio Science Meeting, Atlanta, GA, USA, 7–12 July 2019; pp. 2169–2170.
25. Gólkowski, M.; Park, J.; Bittle, J.; Babaiahgari, B.; Rorrer, R.A.L.; Celinski, Z. Novel mechanical magnetic shutter antenna for ELF /VLF radiation. In Proceedings of the 2018 IEEE International Symposium on Antennas and Propagation & USNC/URSI National Radio Science Meeting, Boston, MA, USA, 8–13 July 2018; pp. 65–66.